Over-damped Dynamics of Single-Chain Flexible and Semiflexible Polymers in Implicit Solvent Conditions

Varun Madan Mohan

A dissertation submitted for the partial fulfillment of BS-MS dual degree in Science

Indian Institute of Science Education and Research Mohali

April 2019

Certificate of Examination

This is to certify that the dissertation titled "Over-damped Dynamics of Single-Chain Flexible and Semiflexible Polymers in Implicit Solvent Conditions" submitted by Mr. Varun Madan Mohan (Reg. No. MS14115) for the partial fulfilment of BS-MS dual degree programme of the Institute, has been examined by the thesis committee duly appointed by the Institute. The committee finds the work done by the candidate satisfactory and recommends that the report be accepted.

Dr. Abhishek Chaudhuri Dr. Rajeev Kapri Dr. Dipanjan Chakraborty

(Supervisor)

Dated: April 25, 2019

Declaration

The work presented in this dissertation has been carried out by me under the guidance of Dr. Dipanjan Chakraborty at the Indian Institute of Science Education and Research Mohali.

This work has not been submitted in part or in full for a degree, a diploma, or a fellowship to any other university or institute. Whenever contributions of others are involved, every effort is made to indicate this clearly, with due acknowledgement of collaborative research and discussions. This thesis is a bonafide record of original work done by me and all sources listed within have been detailed in the bibliography.

Varun Madan Mohan

(Candidate)

Dated: April 25, 2019

In my capacity as the supervisor of the candidate's project work, I certify that the above statements by the candidate are true to the best of my knowledge.

Dr. Dipanjan Chakraborty

(Supervisor)

Acknowledgement

To thank each and every entity of the universe that inspired, guided, or helped me plow through the longer and more difficult days and nights since the commencement of this work, would be a task almost impossible to execute. However to not carve into stone(or paper) the contribution of a few truly special people to my success, sanity, and overall happiness, and my gratitude for the same, would be a sin of galactic proportions.

I will begin by thanking my academic guide, Dr. Dipanjan Chakraborty, whose ever jovial and informal nature rendered him approachable with any conundrum that warranted serious brainstorming. I am ever grateful for the powerful computing resources that he gave me access to, which not only facilitated the efficient execution of most of the work, but also made me adept at computational techniques, and helped me in understanding and handling clusters.
I also thank the Department of Science and Technology of the Government of India, for financially supporting me throughout the period of my BS-MS Programme through the INSPIRE Fellowship.

Moving onto the wonderful individuals for whom "friends" seem too low of a designation, I'd like to first express my love and gratitude towards Awani Bapat, who pretty much created a home for me in IISER and also knows me like the back of her hand, without whom this thesis would most definitely not have existed, as I would most probably have moved to the neighbouring Himalayas to try and find some help to deal with my debilitating anxiety attacks and mood swings.
I would like to thank Priyasha Deshpande, who patiently suffered my stress fuelled passive aggressive episodes despite having done nothing to deserve it, and yet remained an unconditionally loving friend and a shoulder to cry on.
I thank Adarsh Prabhakaran for being the supportive *hype man* who instilled in me the finer skills of the caveman, and transformed me into the hardened street smart (hopefully) individual that I am today.

A group of three is a party by themselves, and my group would be incomplete without Vishnu N Nampoothiri, who has surprisingly remained my friend despite being at the receiving end of relentless yet playful taunts, hurled by Adarsh and I.
I thank Leesa Joyce for being a loving friend, a calm listener, and a colourful story-teller, whose stories deserve a book of their own.
I also thank Richa Singh for the late night coffee breaks and long conversations, and for always checking up whenever she sensed that something was bothering me.
For helping me take my mind off stuff by talking about absolutely any topic under the sun, as well as about pressing matters such as substance abuse, oral hygiene, and medical conditions affecting the oral cavity, I thank my expansive dentist-friend, Dr. Prema Sivakumar (Sakshi).
I also express my deepest love and gratitude to Muskaan, for giving me countless reasons to laugh and smile, even throughout the stressful period leading up to the submission of this thesis.
I will forever be indebted to my family, who recognized my love for science, especially my father for enthusiastically offering to help me with educational resources, my mother for keeping me up-to-date with family gossip, and my brother for the good music and dark humour.

I would also like to put on record my sincerest gratitude to Somak, Shiny, Swetha, Sachin, Vaitheesh, Abin, Balu, Jain, Aswathy, and Adheena, for the good times that will be remembered forever.

The least I can do to express my gratitude to these individuals is to dedicate to them this body of work, which has boiled down from the long hours I've spent exploring the world of polymers.

Varun Madan Mohan

List of Figures

Contents

Abstract

Molecular dynamics simulations are used to study the dynamics of polymers in an implicit solvent, imposed by a Brownian thermostat. The dynamics of the system is reduced to its normal coordinates, and its conformation to the model proposed by Rouse is confirmed by analysing the scaling of normal coordinate correlation relaxation times with monomer and mode number. The scaling is analysed for single Gaussian chains of flexible and semiflexible polymers, with point mass monomers and harmonic bonds. The semiflexible polymer chain is subjected to a normal coordinate decomposition identical to that employed in the flexible case, which has been found to hold in the limit of low bending rigidity. It is also found that the introduction of explicit solvent particles and implementation of a dissipative particle dynamics (DPD) thermostat shifts the scaling of normal coordinate relaxation times towards the theoretical value predicted by the Zimm model, suggesting the introduction of effective hydrodynamic interactions. The clustering effects induced by introducing type-dependent deep potential wells(patches) along a heterogeneous polymer chain is also studied. Attractive patches have also been introduced randomly along rigid semiflexible polymer chains, which has been found to result in the decrease of the chain's persistence length.

Chapter 1

Introduction

From plastics and rubber to DNA and proteins, polymers are ubiquitous. Whether they are artificially synthesised or naturally occurring, polymers are interesting large, high molecular weight entities with a connected structure of usually a large number of monomers, as boldly proposed by Staudinger(Staudinger 20) in 1920. The inter- and intra- chain interactions of monomers result in properties that may be completely disconnected from their monomeric units. A tangible example would be the extent of differences between the sweet smelling quickly evaporating organic molecule styrene, which when polymerized produces the well known polystyrene, which is valued for its shock resistant properties. Polymers can be of a single monomer type, like polystyrene, which is made up of styrene monomers, or heterogeneous with respect to monomer types, like the naturally occurring chitin. They can also show crosslinking, facilitated by special monomers along the chain, or by accessory molecules such as Actin-binding proteins(ABPs) which also act as facilitators(Dos Remedios 03). The structural integrity attributed by crosslinking sees considerable representation of such crosslinked polymeric networks in cellular settings, such as in the cytoplasm and the extra-cellular matrix, where structural rigidity is critical for maintaining cell morphology. Monomers in principle can contain any number of atoms, and the constituent atoms and bonds can endow it with effective physical limitations which manifest itself as angular, torsional, and charge-based constraints. Abstracting a polymer to a chain of monomers whose dynamics conform to these constraints allow for a *coarse-grained* understanding of its dynamics. The polymer chain's interactions with itself

and neighbouring chains result in behaviour that is uncommon in liquids such as methanol, water, acetone etc. One such characteristic is the *glass transition* of polymers below a critical temperature to amorphous *glasses*, and its existence as a liquid consisting of thermally agitated chains at temperatures above it. Polymeric liquids however, do not exactly behave like substances such as water even at temperatures above the glass transition temperature. Natural and artificial polymeric substances around us such as chewing gum, latex, starch etc. behave like water in that they fill the volume of a container of any shape, but at the same time, can exhibit properties such as elasticity when subjected to sudden deformations. Polymeric liquids are also viscous, and the properties of viscosity and elasticity are termed together as *viscoelasticity*. The origin of this viscoelastic nature lies in the constituents of the liquid, which are the interacting polymer chains. Polymers can also undergo a partial crystallization as opposed to a pure glass transition. The semicrystalline polymers are generally more thermally stable and harder than purely glassy polymers, but the crystalline regions tend to be more brittle(Seymour 03).

The scale of advancement computational techniques have blessed the field of theoretical polymer physics with cannot be underestimated. The advent of faster processors, powerful graphics processing units(GPU), simulation packages such as the Large-scale Atomic/Molecular Massively Parallel Simulator(LAMMPS), HOOMD-Blue, Nanoscale Molecular Dynamics(NAMD) etc. and visualization tools such as Visual Molecular dynamics(VMD) have revolutionized research capabilities, and have helped push the limits of modelling towards large systems with particle numbers even of the order of 10^{12}. Polymers are usually modelled by a coarse grained approach, where they are reduced to a "bare minimum" of functional entities, required for the system to behave like the polymer in question. Understanding the dynamics of even a single polymer chain is a complex problem as it represents a system of interacting particles. The interactions can be broadly classified into bonded and non-bonded interactions, where the bonded category contains bonding, bending and torsional potentials, and the non bonded interactions include potentials like Lennard-Jones (LJ), electrostatic, magnetic etc. A common method of analysing dynamics of single-chain systems is to decompose it its normal coordinates, so as to obtain independent solu-

tions to the differential equation(DE) that governs its dynamics; a technique which will extensively be used in the work documented in this thesis.

1.1 Langevin and Brownian Dynamics

A molecular scale model of a system such as that of a polymer in a solvent must incorporate terms that take collisions of thermally agitated solvent particles with those of the polymer into account. The Langevin equation, which is a stochastic DE can be used for modelling such systems(Langevin 08). The stochastic part of the DE mimics the random collisions of the solvent with the particles of interest. It must be noted that Langevin dynamics is an implicit solvent approximation. This equation also takes the viscosity of the solvent into consideration, and implements it through a *drag* term. Temperature of the setup is contained as a linear scaling factor in the stochastic force term, and translates to an increase in the strength of random collisions as the temperature of the solvent is increased. By acting as a thermostat, the Langevin dynamics implementation effectively samples a canonical ensemble. The Langevin equation for a particle at position $\mathbf{x}$, in a solvent of viscosity η, at temperature T is:

$$m\ddot{\mathbf{x}} = -\nabla U(\mathbf{x}) - \eta\dot{\mathbf{x}} + \mathbf{r}(t). \tag{1.1}$$

Here, η is the product of the mass,m, by γ, which is the inverse of the damping time. The damping time is effectively the amount of time it takes for the energy of the particle to be dissipated. $\mathbf{r}(t)$ is a delta correlated random vector, which is nowhere differentiable, whose integral is a Wiener process. $U(\mathbf{x})$ is the potential at the point $\mathbf{x}$, and contains all bonded and non-bonded potentials, $U = U_{bonded} + U_{non-bonded}$.

$$\left\langle \mathbf{r}(0) \cdot \mathbf{r}(t) \right\rangle = 2m\gamma k_B T\delta(t). \tag{1.2}$$

The Langevin equation can be simplified to a first-order DE, by assuming that the dynamics is over-damped. In this regime, $\gamma \longrightarrow \infty$ since the damping time approaches zero. Over-damped Langevin dynamics is known as Brownian dynamics, and is used in all the simulations, unless specified otherwise. The equation for Brownian dynamics,

along with those leading up to it are as follows:

$$m\ddot{\mathbf{x}} = -\nabla U(\mathbf{x}) - \eta\dot{\mathbf{x}} + \mathbf{r}(t) \tag{1.3}$$

$$\dot{\mathbf{x}} = -\frac{1}{m\gamma}\nabla U(\mathbf{x}) + \frac{1}{m\gamma}\mathbf{r}(t),\ since\ \gamma \longrightarrow \infty \tag{1.4}$$

Acceleration of a particle is not defined in a Brownian regime, and thus the integration technique used will be different from the standard velocity-Verlet algorithm. This technique, called the Euler-Maruyama algorithm, will be addressed in the Chapter 5.

1.2 Dissipative Particle Dynamics

As mentioned in the previous section, the Langevin equation assumes an implicit solvent, and is thus a rather simplified approximation of the solvent. While not assuming the existence of explicit solvent particles is computationally favourable, a more realistic representation of the system demands the use of explicit solvent particles. Moreover, the Langevin equation does not contain a term that accounts for hydrodynamic interactions, which exist in most dense solvents. Although these properties can be incorporated by using special potential terms, as will be elaborated in sect.2.3 on the Zimm model, a Dissipative Particle Dynamics (DPD) thermostat has been found to result in Zimm like scaling, for simulations of flash nanoprecipitation of block copolymers(Spaeth 11), which motivated a probing of this shift in scaling for single flexible polymer chains(sect.2.3). The DPD equation of motion by construction, contains a dissipative force term, a conservative soft repulsive force, and an impulsive random force(Groot 97). The DPD equation is:

$$\mathbf{f}_i = \sum_{j\neq i}\left(\mathbf{F}_{ij}^C + \mathbf{F}_{ij}^R + \mathbf{F}_{ij}^D\right) \tag{1.5}$$

$$\mathbf{F}_{ij}^C = a_{ij}\left(1 - \frac{r_{ij}}{r_c}\right)\hat{\mathbf{r}}_{ij} \tag{1.6}$$

$$\mathbf{F}_{ij}^R = \frac{\sigma_{ij}\theta_{ij}}{\sqrt{\Delta t_D PD}}\left(1 - \frac{r_{ij}}{r_c}\right)\hat{\mathbf{r}}_{ij} \tag{1.7}$$

$$\mathbf{F}_{ij}^{D} = -\gamma_{ij}\left(1 - \frac{r_{ij}}{r_c}\right)^2 \left(\hat{\mathbf{r}}_{ij} \cdot \mathbf{v}_{ij}\right)\hat{\mathbf{r}}_{ij} \tag{1.8}$$

Here, a_{ij} is the maximum repulsion between particles i and j, located at $\mathbf{r}_i$ and $\mathbf{r}_j$ respectively. $\hat{\mathbf{r}_{ij}} = (\mathbf{r}_i - \mathbf{r}_j)/r_{ij}$, and $\mathbf{v}_{ij} = \mathbf{v}_i - \mathbf{v}_j$ is the relative velocity of particle i with respect to particle j. θ_{ij} is a Gaussian random number with unit variance and zero mean. σ_{ij} is called a noise parameter, and follows:

$$\sigma_{ij}^2 = 2m\gamma_{ij}k_BT.$$

γ_{ij} is the friction coefficient, and similar to γ in the Langevin dynamics paradigm. Comparing the above with eqn.1.2 shows that the random force, $\mathbf{r}(t) \equiv \sigma\theta(t)$. The values of γ, σ, and a can be set for different particle types, and thus will effectively represent interactions between solvent particles and particles of the system.

1.3 Flexible Polymers

A polymer chain is termed flexible, when it has no bond rotational constraints. This absence of bending or torsional rigidity subsequently implies that the bonded part of the total potential, U_{bonded}, consists only of a bond potential(rigid, harmonic, FENE etc.). A flexible polymer is the simplest case of a connected system of monomers and has been statistically analysed using rigid-bond models such as the *freely jointed chain* and *freely rotating chain*. The *Gaussian chain*(GC) model, which assumes bond lengths to be normally distributed about an equilibrium displacement, can also be used for modelling flexible polymers. The GC model is similar to one which assumes harmonic bonds to exist between monomers, and is also called the *bead-spring* model. Thus, this model can also be viewed as an N-mass-and-spring system. The mathematical simplicity of this model allows for a straightforward normal coordinate formulation of the polymer chain, which will be elaborated on in Chapter 2.

1.4 Semiflexible Polymers

The introduction of bending rigidity to an otherwise flexible polymer manifests as properties that can be observed in both single chains, as well as polymer networks. These polymers are called *semiflexible polymers*. Semiflexible polymers have an angle dependent term in its Hamiltonian, which imposes an energetic cost on bending. Thus, these polymers tend to maintain a straight conformation, provided that the thermal fluctuations are minimal. A model for such polymers is called the Wormlike chain(WLC) model, which is a continuous form of a model first proposed by Kratky and Porod(Kratky 49). The Kratky-Porod (WLC) model has also been used in the analysis of DNA(Marko 95)(Jian 97)(Mazur 07) and charged polyelectrolytes (Skolnick 77). A variant of the WLC model with a stretched relaxation spectrum, called the glassy wormlike chain (GWLC), has also been formulated, and has been found to predict mechanical observables conforming to those observed in cell and reconstituted cytoskeletal systems(Kroy 07).

The *persistence length*, which is defined as the distance after which the correlation between tangent vectors vanishes, is a measure which reflects the stiffness of the polymer. Unlike the case of flexible polymers, the bending rigidity that is introduced makes normal coordinate decomposition rather difficult, and thus, techniques employed for the flexible polymer case work only as an approximation in the semiflexible case. These issues are addressed in detail in Chapter 3. What makes semiflexible polymers an important research topic is the representation of these polymers in biological systems, especially at the cellular level. The cytoskeletal protein *globular* actin, or G-actin, polymerizes to form *filamentous* actin, or F-actin, which is a semiflexible polymer. Another cell-scale semiflexible polymer is collagen, which is present in the extra-cellular matrix. The role of F-actin in maintaining the cell's morphology could not have been executed effectively had it been a flexible polymer, since flexible polymers cannot form rigid networks because of the absence of chain stiffness. F-actin has a persistence length which is comparable to its usual contour length, whereas microtubules, another kind of cytoskeletal proteins, are much more rigid, with the persistence length about 10^2 times the contour length(Broedersz 14). The

elastic response of semiflexible polymers is non-trivial and depends strongly on the ratio between persistence and contour lengths, with the maximum response shown by polymers with persistence lengths of the order of contour lengths, as is the case with F-actin. The response also changes from being isotropic(independent of the angle of force application) when the ratio is less than 1, to being anisotropic(angle dependent response) as the ratio approaches and goes beyond 1(rigid polymers)(Kroy 96). The elastic properties of semiflexible polymers have also been found to be ensemble dependent, with constant-extension ensembles showing qualitative differences in properties when compared to constant-force ensembles(Dhar 02). The viscoelastic properties of semiflexible biopolymers can also been probed using single-molecule techniques, such as Fluorescence Resonant Energy Transfer(FRET), through the correlation function of single molecules(Yang 02). The use of single-polymer measurement techniques of such properties is termed as microrheology.

1.5 Rouse and Zimm Models

The dynamics of polymers in a solution by studying the Brownian motion of the monomers was first proposed by Rouse(Rouse Jr 53). Rouse employed the bead-spring model, where the equations of motion of the monomers was given by the Langevin equation, in the over-damped Brownian limit. The Rouse model is a physically simple model, which, in theta conditions, does not take into consideration excluded volume interactions. Most importantly, it also disregards the hydrodynamic interaction. The latter results in certain discrepancies in the light of empirical data, which will be addressed in Chapter 2. The shortcomings of the Rouse model were overcome by Zimm's model, which made the important change to the mobility tensor to account for hydrodynamic interactions, which plays a considerable role in polymer dynamics in dense solutions(Zimm 56). The introduction of explicit solvent particles in a Langevin thermostat has also been found to result in conformation to the Zimm model's predictions(Dünweg 93), similar to the DPD approach studied in this work.

1.6 Many chain systems and polymer networks

The interesting dynamical properties of single polymer chains lead to a variety of novel phenomena when the concentration of such entities increase, or the polymer chains are fixed by crosslinking to form networks. The single-chain case can be assumed to be the vanishingly dilute limit of the polymer solution. With the increase in concentration, many-chain effects manifest as changes in the dependence of macroscopic quantities (such as the osmotic pressure(Noda 81)) on the chain concentration(Doi 88). Semiflexible polymers, whose dynamics depend strongly on its stiffness, can form rigid crosslinked networks, especially in biological systems, with network properties such as elastic moduli which depend on crosslinking density, mesh size, and persistence length of the constituent polymer chains. The stress-response of the network and the spatial distribution of microscopic deformations have also been found to be dependent on the relative magnitudes of the bending force and bond force constants(Head 03), thereby linking the microscopic properties of the individual polymer chains with macroscopic phenomena. The difficulty in the analytical treatment of semiflexible polymer chains is experienced not only in the single-chain, but also in many-chain systems. In the highly concentrated (tightly entangled) regime (i.e. mesh size smaller than persistence length), experimental observations were found to directly contradict with prior theories pertaining to the dependence of the plateau modulus to chain and solution parameters(Schuldt 16). This was further corroborated by Tassieri(Tassieri 17) in the light of previous findings(Tassieri 08a)(Tassieri 08b). A comprehensive theory of many-chain semiflexible polymer systems is yet to be formulated.

Chapter 2

Flexible Polymers

2.1 The Rouse model

Let a flexible polymer consist of N monomers, whose position vectors are given as $\mathbf{R}_n$ ($n \in \{1, 2, ..., N\}$), and be subjected to a Brownian thermostat. The Brownian equation can be written in the form of the Smoluchowski equation (given that the diffusion constant is position independent)(Lax 60) as,

$$\frac{\partial \mathbf{R}_n(t)}{\partial t} = \sum_m \mathbf{H}_{nm} \cdot \left(\frac{-\partial U}{\partial \mathbf{R}_m} + \mathbf{f}_m(t) \right) + \frac{1}{2} k_B T \sum_m \frac{\partial}{\partial \mathbf{R}_m} \cdot \mathbf{H}_{nm} \tag{2.1}$$

The mobility tensor defines the relationship between the velocity of a particle n and the force applied on it by all other particles.

$$\mathbf{v}_n = \sum_m \mathbf{H}_{nm} \cdot \mathbf{F}_m \tag{2.2}$$

For the Rouse model, hydrodynamic interactions and excluded volume interactions are not considered. The latter can be justified by assuming Θ condition. The absence of hydrodynamic interactions is encoded in the mobility tensor, which, for the Rouse model, has the form:

$$\mathbf{H}_{nm} = \frac{\mathbf{I}}{\zeta} \delta_{nm}$$

where ζ is the drag coefficient, $m\gamma$. Using the Rouse approximation of the mobility tensor, the Brownian equation takes the simple continuous form:

$$\zeta \frac{\partial \mathbf{R}_n(t)}{\partial t} = \frac{-\partial U}{\partial \mathbf{R}_n} + \mathbf{f}_n(t), \tag{2.3}$$

similar to eqn.1.3. In the under-damped regime, the Rouse model equation takes the form:

$$m\frac{\partial^2 \mathbf{R}_n(t)}{\partial t^2} = \frac{-\partial U}{\partial \mathbf{R}_n} - m\gamma \frac{\partial \mathbf{R}_n(t)}{\partial t} + \mathbf{f}_n(t) \tag{2.4}$$

where m is the mass of the monomer, γ is the *kinematic viscosity* of the solvent, in units of $time^{-1}$, which is equivalent to the inverse of damping time as mentioned in sect.1.1, and $m\gamma$ is the drag coefficient ζ. In eqn.2.3 and eqn.2.4, $\mathbf{f}_n(t)$ is a random Gaussian force($\mathbf{f}_n \equiv \mathbf{r}(t)$ in sect.1.1) with the properties:

$$\big\langle \mathbf{f}_n(t) \big\rangle = 0$$

$$\big\langle \mathbf{f}_n(0) \cdot \mathbf{f}_m(t) \big\rangle = 2m\gamma k_B T \delta_{nm} \delta(t). \tag{2.5}$$

The bond potential used is a harmonic potential of the form:

$$U_i^{bond} = k\big(|\mathbf{R}_{i+1} - \mathbf{R}_i| - b\big)^2 \tag{2.6}$$

where b is the equilibrium bond length, and k is the force constant. If we assume each bonded segment to be of a vanishingly small length, the polymer can be approximated to a space curve parameterised by n. In the continuous limit, the Brownian equation for the bead spring model takes the form:

$$\zeta \frac{\partial \mathbf{R}_n(t)}{\partial t} = k\frac{\partial^2 \mathbf{R}_n(t)}{\partial n^2} + \mathbf{f}_n(t) \tag{2.7}$$

The harmonic term is a second derivative with respect to the parameter n, and will clearly reflect the nearest bonded neighbour interaction, as mentioned above, when discretised. In order to overcome this interaction terms, normal coordinates are employed, as will be shown in the next section.

2.2 Normal coordinates

Since the flexible polymer represents an N-interacting system, whereby the force on a particle i depends on the positions of the $i-1$ and $i+1$ particles, solutions to the DE capable of independent motion are the normal coordinates of the system. The normal coordinates of the polymer is given by(Doi 88):

$$\mathbf{X}_p \equiv \frac{1}{N}\int_0^N dn \cos\left(\frac{p\pi n}{N}\right)\mathbf{R}_n(t) \; with \; p = 0, 1, 2, ... \tag{2.8}$$

This can be discretized to give:

$$\mathbf{X}_p(t) = \frac{1}{N}\sum_{n=0}^{N-1}\mathbf{R}_n(t)\cos\left(\frac{p\pi}{N}\left(n+\frac{1}{2}\right)\right) \tag{2.9}$$

The normal coordinates, when applied to the continuous form of the Brownian equation reduces it to a first order DE, of the simple form:

$$\zeta_p\frac{\partial \mathbf{X}_p(t)}{\partial t} = k_p\mathbf{X}_p(t) + \mathbf{f}_p(t) \tag{2.10}$$

Where ζ_p and k_p are the effective drag coefficient and force constant respectively. The exact form of these quantities are dependent on whether the polymer is observed from its center of mass frame or not (Refer Chapter 5). However, the scaling of these quantities with N and p holds true for both frames of reference, and for the Rouse model, $k_p \propto p^2$, $k_p \propto 1/N$, and $\zeta_p \propto N$. Using $\mathbf{X}_p$, the positions of the monomers are given as:

$$\mathbf{R}_n = \mathbf{X}_0 + 2\sum_{p=1}^{\infty}\mathbf{X}_p\cos\left(\frac{p\pi n}{N}\right) \tag{2.11}$$

All quantities depending on the positions of the monomers can be converted into the normal coordinate form and the correlation of these functions can give an insight into the normal mode timescales that are contained in it. From eqn.2.10, eqn.2.5, and remembering that the $\mathbf{X}_p$s are capable of independent motion, we get the general normal coordinate correlation:

$$\langle \mathbf{X}_{p\alpha}(0)\cdot\mathbf{X}_{q\beta}(t)\rangle = \delta_{pq}\delta_{\alpha\beta}\frac{k_BT}{k_p}e^{\frac{-t}{\tau_p}}, \tag{2.12}$$

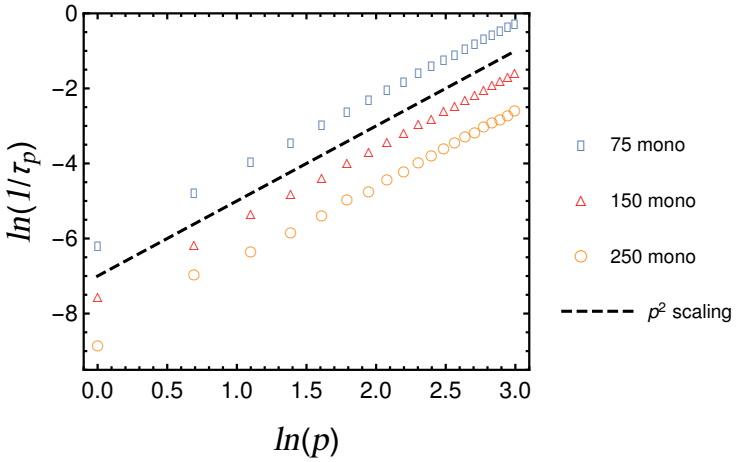

Figure 2.1: $\ln(1/\tau_p)$ as a function of $\ln(p)$ for the first 20 modes, for flexible polymers of different lengths. They all follow the Rouse scaling given by $\tau_p \sim p^{-2}$ (see eqn.2.13), irrespective of monomer number.

Where τ_p is the relaxation time of the p^{th} normal mode, and is related to the first normal mode, which is also the longest mode, by:

$$\tau_p = \frac{\tau_1}{p^2} \tag{2.13}$$

$$\tau_1 = \frac{\zeta_1}{k_1}. \tag{2.14}$$

This scaling of τ_p with p^{-2} can be clearly seen for polymers of various lengths in Fig.2.1. The inverse quadratic scaling gets altered with the introduction of even a slight bending rigidity, and can thus be means of distinguishing flexible polymers from semiflexible ones. This will be addressed in Chapter 3. Another clear-cut distinction between flexible and semiflexible polymers can be obtained by looking at the mean-square mode amplitude $\langle \mathbf{X}_p^2(0) \rangle$, which for flexible polymers is given as:

$$\langle \mathbf{X}_p^2(0) \rangle = \frac{k_B T}{k_p} \implies \langle \mathbf{X}_p^2 \rangle \propto p^{-2} \tag{2.15}$$

The p^{-2} dependence is shown in Fig.2.2, for various monomer numbers. However, when a bending rigidity is introduced, the p dependence of the mean-square mode amplitude changes drastically (Refer eqn.3.10 and Fig.3.3). Plotting the ratio of the log of the correlation given by eqn.2.12 to time, $\ln\langle \mathbf{X}_p(t) \cdot \mathbf{X}_p(0) \rangle / t$, as a function of time, reflects the relaxation time of the normal coordinate correlation, when it assumes a constant value. This can be seen in Fig.2.3, where the inverse of correlation

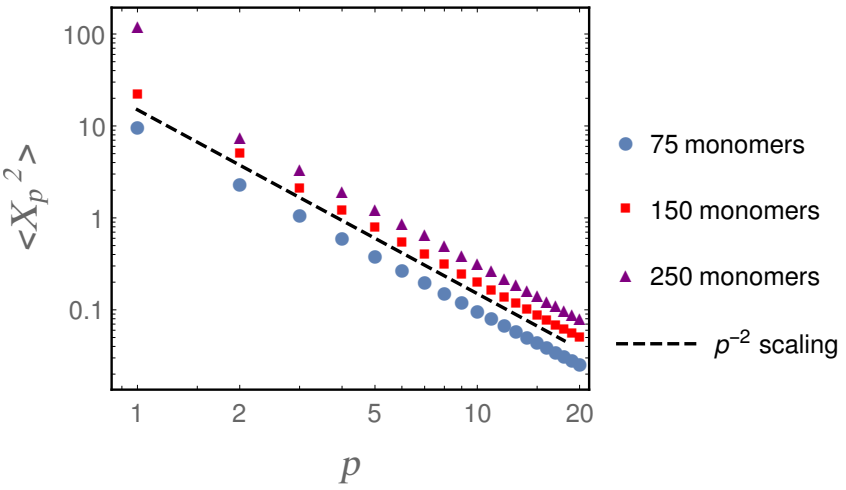

Figure 2.2: $\langle \mathbf{X}_p^2(0) \rangle$ as function of p, for polymers of various lengths. The p^{-2} scaling is as predicted by the Rouse model of a flexible polymer chain (see eqn.2.15).

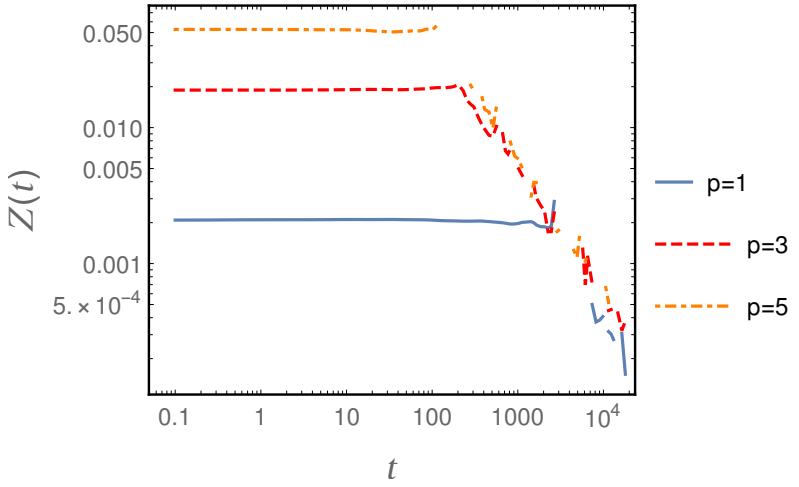

Figure 2.3: Plot of $Z(t) = \ln\langle \mathbf{X}_p(t) \cdot \mathbf{X}_p(0) \rangle / t$ as a function of t, for a 75 monomer long flexible polymer and p=1,3,5. The value of $Z(t)$ at the plateaus is equal to $1/\tau_p$.

relaxation times($1/\tau_p$) of the normal coordinates 1, 3, and 5 are the $Z(t)$ values at the plateau-like regions in the plot. The breaks in the plot correspond to the correlation assuming negative values, for which the logarithm is not defined.

The correlation time of the end-to-end vector can be derived by writing it in terms of normal coordinates, and using eqn.2.12:

$$\mathbf{P}(t) = \mathbf{R}_N(t) - \mathbf{R}_0(t)$$

$$\mathbf{P}(t) = -4 \sum_{p:odd} \mathbf{X}_p(t)$$

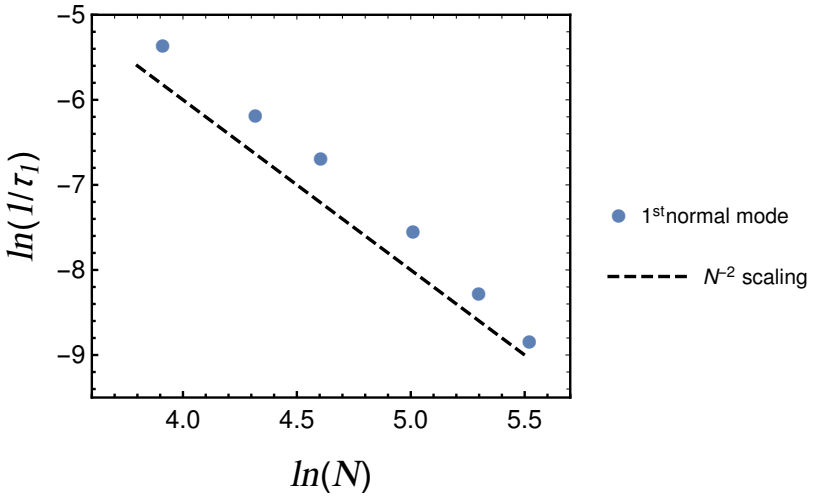

Figure 2.4: $\ln(1/\tau_1)$ as a function of $\ln(N)$. This reveals the scaling of $1/\tau_1$ with N, which follows well with the Rouse model prediction.

$$\langle \mathbf{P}(t) \cdot \mathbf{P}(0) \rangle = -16 \sum_{p:odd} \langle \mathbf{X}_p(t) \cdot \mathbf{X}_p(0) \rangle$$

$$\langle \mathbf{P}(t) \cdot \mathbf{P}(0) \rangle = -16 \sum_{p:odd} \frac{3k_B T}{k_p} e^{\frac{-t}{\tau_p}} \tag{2.16}$$

From the eqn.2.16, the maximum contribution to the end-to-end vector correlation relaxation time comes from the first normal mode, and the successive modes have contributions which decrease rapidly, which follows from eqn.2.13 . The longest relaxation time of $\langle \mathbf{P}(t) \cdot \mathbf{P}(0) \rangle$ is called the rotational relaxation time τ_r of the polymer. This relaxation time is equal to τ_1, and from eqn.2.14, it is predicted that $\tau_r \equiv \tau_1 \propto N^2$, for the Rouse model. This trend can be clearly observed in Fig.2.4. This scaling however, is not experimentally observed for dilute solutions in Θ conditions, since the assumption of absence of hydrodynamic interactions is erroneous. This discrepancy was theoretically tackled by Zimm, whose model will be discussed in the next section.

2.3 The Zimm model

The purpose of this Brownian dynamics theoretical elaboration of this model is purely to round off the discussion on the Rouse model by introducing the hydrodynamic interaction term in the mobility tensor. This approach is not implemented in this work, but the results are rather arrived at using an explicit solvent and a DPD thermostat.

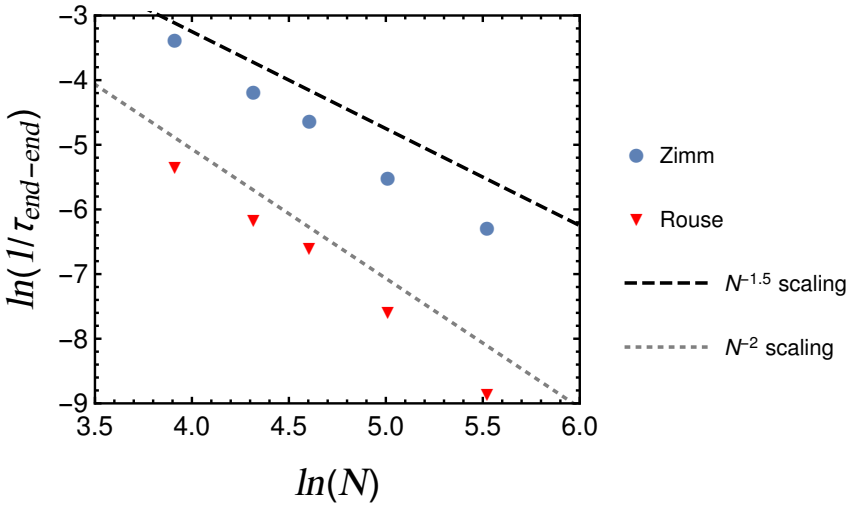

Figure 2.5: $\ln(1/\tau_{end-end})$ as a function of $\ln(N)$, with dashed lines corresponding to Rouse(N^{-2}) and Zimm($N^{-1.5}$) scaling. The Rouse model conforming data is for the implicit solvent devoid of hydrodynamic interactions, and the data for the Zimm model is for explicit solvent case, with the DPD thermostat.

As mentioned in the previous section, the Rouse model does not take into consideration hydrodynamic interactions, which are capable of affecting the dynamics of polymer chains, especially in dense media. The hydrodynamic interaction is, simply put, a "push" experienced by particles around a particle that experiences some force which causes its motion. This interaction depicts a dispersion of energy among neighbours, centered along the line of contact. The mobility tensor defines a velocity field, in response to a force, as given in eqn.2.2. The difference to the Rouse model introduced by Zimm was in the mobility tensor term, which was changed from $\mathbf{H}_{nm} = \mathbf{I}\delta_{nm}/\zeta$ to:

$$\mathbf{H}_{nn} = \frac{\mathbf{I}}{\zeta}$$

$$\mathbf{H}_{nm} = \frac{1}{8\pi\eta_s|\mathbf{r}_{nm}|}\left[\hat{\mathbf{r}_{nm}}\hat{\mathbf{r}_{nm}} + \mathbf{I}\right] \; for \; n \neq m$$

Here, η_s is the viscosity of the solvent, and $\mathbf{r}_{nm} = \mathbf{R}_n - \mathbf{R}_m$. For this term of the mobility tensor,

$$\frac{\partial}{\partial \mathbf{R}_m} \cdot \mathbf{H}_{nm} = 0$$

Thus, from eqn.2.1, we get the Brownian equation for a general mobility tensor,

$$\frac{\partial \mathbf{R}_n(t)}{\partial t} = \sum_m \mathbf{H}_{nm} \cdot \left(\frac{-\partial U}{\partial \mathbf{R}_m} + \mathbf{f}_m(t)\right)$$

For the Θ condition, in the continuous limit, we obtain the Zimm model equation(Zimm 56),

$$\frac{\partial \mathbf{R}_n(t)}{\partial t} = \sum_m \mathbf{H}_{nm} \cdot \left(k \frac{\partial^2 \mathbf{R}_n(t)}{\partial n^2} + f_m(t) \right) \tag{2.17}$$

We can see that the major difference between the mathematical forms of the Rouse and Zimm model lies in the summation over the product with the elements of the mobility tensor. The same normal coordinates used in the Rouse model are used in this model and predicts a rotational relaxation time $\tau_r \propto N^{3/2}$.

As mentioned in sect.1.2, a DPD thermostat can be employed to mimic a realistic system with explicit solvent particles, which can interact purely by a soft repulsion, along with separate stochastic and dissipative terms. Employing a DPD thermostat for the single flexible chain case, along with explicit solvent particles, shifts the scaling of the correlation relaxation times of the end-to-end vector from a Rouse scaling, as N^2, towards a less steep Zimm scaling of $N^{3/2}$. This shift in scaling, although subtle, can be seen in Fig.2.5. A possibly better shift to Zimm scaling might be observed at higher solvent particle densities, ρ, which is 1 in this case. The dynamics of the system should also depend on the parameters of the DPD thermostat used, such as the maximum repulsive force, a_{ij}, and the cutoff, r_c.

Chapter 3

Semiflexible Polymers

3.1 The Semiflexible Hamiltonian

Semiflexible polymers are different from their flexible counterparts, in that a bending rigidity is introduced in its Hamiltonian, which imposes an energetic cost to bending, thus rendering these polymers approximately straight up to a certain *persistence length*, at non zero temperatures. The model for semiflexible polymers was published in 1949 by Kratky and Porod(Kratky 49), which has since been mathematically idealised to a continuous model called the wormlike chain (WLC) model. Unlike purely flexible polymers, which try to maximize conformational entropy, there is an optimization between entropic and energetic costs in the case of semiflexible polymers.

3.2 Kratky-Porod Model

The Kratky-Porod model assumes a polymer chain with bonds of a fixed length l, and a bending rigidity that favours a straight conformation. The bending potential is given as:

$$U_{bend} = \kappa \sum_{i=2}^{N-1} (1 + \cos \vartheta_i) \tag{3.1}$$

Where ϑ_i is the bond angle between the two bonds that meet at monomer iThe Kratky-Porod equation, which gives $\langle R^2 \rangle$ as a function of the separation between

monomers and is also one of the few analytical relations pertaining to this model, is arrived at from the freely rotating chain model. As a measure of stiffness, we look at how a bond vector(say the first), $\mathbf{l}_1$ is oriented with respect to the end to end vector, $\mathbf{R}$:

$$\frac{\langle \mathbf{R} \cdot \mathbf{l}_1 \rangle}{l} = \sum_{j>1}^{\infty} \langle \cos(\theta_{1,j}) \rangle.$$

For a stiff polymer the angle of deviation would be close to zero. In the long chain limit ($L, N \longrightarrow \infty$) the above reduces to the definition of the persistence length:

$$l_p = \frac{l}{1 - \cos(\theta)} \approx \frac{-l}{\ln\big[\cos(\theta)\big]} \tag{3.2}$$

The mean square end-to-end vector of this model is:

$$\frac{\langle R^2 \rangle}{Nl^2} = \frac{1 + cos(\theta)}{1 - \cos(\theta)} - \frac{2\cos(\theta) + \cos^{N+1}(\theta)}{N[1 - \cos(\theta)]^2}$$

substituting the expression for the persistence length into the above, we get,

$$\langle R^2 \rangle = Nll_p[1 + cos(\theta)] - l_p^2 2\cos(\theta)[1 - \cos^N(\theta)]$$

For small angles, we can use the Taylor series expansion of $\cos(\theta)$ and truncate it after the quadratic terms. Thus,

$$\cos^N(\theta) \approx \left(1 - \frac{\theta^2}{2}\right)^N \approx e^{\frac{-N\theta^2}{2}} = e^{-L/l_p}$$

Assuming a vanishingly small bond length converts the discrete polymer model to an inextensible space curve, parametrised by the arc length. In this limit, $N \longrightarrow \infty$, $l \longrightarrow 0$ and $L = Nl$. Using this and the $\cos^N(\theta)$ approximation in the expression for $\langle R^2 \rangle$, we get the Kratky-Porod equation:

$$\langle R^2 \rangle = 2Ll_p - 2l_p^2[1 - e^{-L/l_p}] \tag{3.3}$$

The equation above can be used to determine the persistence length of a polymer chain from experimental data, among other techniques(Zhang 19). This technique has been employed in finding the persistence lengths of DNA(Beuwer 16)(Kang 17).

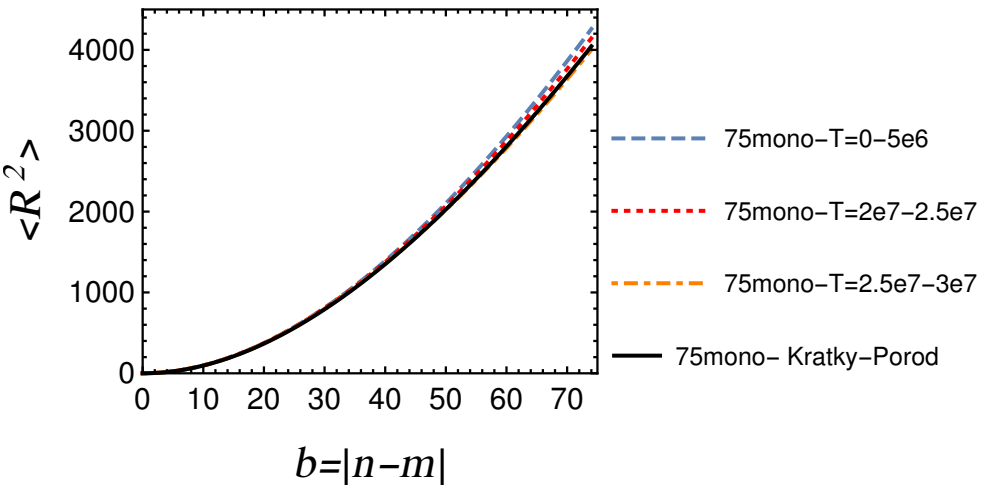

Figure 3.1: Mean square bond length distribution, $\langle R^2 \rangle$, as a function of monomer index separation, $b = |n - m|$. Each curve corresponds to an average over the polymer chain, and over 5×10^6 timesteps, at three different intervals. The distribution progressively conforms to the Kratky-Porod prediction, with later intervals.

It can also be clearly seen from the equation above, how the semiflexible polymer case can give the rigid rod and flexible polymer as limiting cases:

$$\langle R^2 \rangle = L^2 \ for \ L/l_p \longrightarrow 0 \ (Rigid \ rod)$$

$$\langle R^2 \rangle = 2Ll_p \ for \ L/l_p \longrightarrow \infty \ (Flexible \ chain)$$

The ratio of contour length to the persistence length is used as a measure of polymer stiffness. For a general $b = |n - m|$ where n and m are monomer indices, we get the more general equation:

$$\langle R^2 \rangle(b) = 2bll_p - 2l_p^2[1 - e^{-bl/l_p}] \tag{3.4}$$

In (Auhl 03), the Kratky-Porod equation is used as an equilibration criterion. This conformation to eqn.3.4 is clearly seen in Fig.3.1, where the time averages over later intervals coincide with the Kratky-Porod prediction, suggesting the equilibration of the polymer chain. In the continuous analogue of the Kratky-Porod model, the WLC model, the bond vectors are equivalent to the tangent vectors located at each point on the curve. The energy functional, which is quadratic in the local curvature is given as:

$$H = \kappa \int_0^L dn (\frac{\partial \mathbf{t}}{\partial \mathbf{n}})^2 \tag{3.5}$$

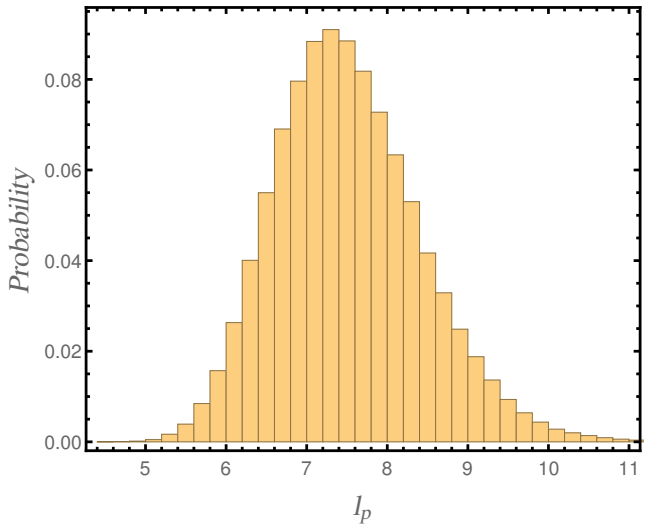

Figure 3.2: Probability distribution of l_p of a 75 monomer long polymer chain, with $\kappa = 7.5$, at $k_BT = 1$. The mean value of the persistence length is, $l_p = 7.516$, which is close to the theoretical l_p, which is 7.5.

where $\mathbf{t}(s) = \frac{\partial \mathbf{r}}{\partial n}$ is the tangent vector at s. The persistence length is also defined as the distance over which the correlations between tangent vectors vanishes. This is given by:

$$\langle \mathbf{t}(n) \cdot \mathbf{t}(n') \rangle = e^{-|n-n'|/l_p}.$$

Fig.3.2 shows the distribution of persistence lengths, computed based on eqn.3.2. The theoretical value of persistence length for a polymer chain with bending rigidity κ at a temperature T, is given by $l_p = \kappa/k_BT$. The persistence length distribution in Fig.3.2 is centered close to 7.5, which also is the value of κ/k_BT. However, it is found that the simulation based value of persistence length does not conform to κ/k_BT for higher values of κ. The causes and dependencies of the same are yet to be probed. A recent publication by Zhang and colleagues(Zhang 19), which lists various methods of extracting information about persistence length from simulation data, also report a deviation of simulation data, from theoretical predictions.

3.3 Normal mode analysis

The analytically exact results pertaining to the WLC model are only in the limits of rigid rods or flexible polymers. Steinhauser proposed a normal coordinate decompo-

sition of the semiflexible polymers(Steinhauser 08), similar to that used in the case of flexible polymers(Doi 88), in the limit of small l_p/L. The application of Hamilton's principle to eqn.3.5, to get the bending force(Harnau 96), is given as,

$$\mathbf{F}^B(n,t) = -l_p k_B T \frac{\partial^4}{\partial n^4}\mathbf{r}(n,t)$$

and will give a 3 particle bond dependent term when discretized (Doi 88). Although the WLC model assumes an inextensible chain, which can be imposed by the condition $|\mathbf{t}(s)| = 1$, Steinhauser uses the bend-resisting force as an extension to the Rouse model for a bead-spring model, and thus, in the continuous limit, results in an equation similar to eqn.2.7 with the added term for the bending force. This method is derived from Harnau, who arrives at this form by applying Hamilton's principle to the Lagrangian of the polymer, which, after substituting for the Lagrangian multipliers, results in the equation of motion at point $\mathbf{r}(n,t)$,

$$\zeta\frac{\partial \mathbf{R}(n,t)}{\partial t} = \frac{3k_BT}{2l_p}\frac{\partial^2\mathbf{R}(n,t)}{\partial n^2} - \frac{3k_BTl_p}{2}\frac{\partial^4\mathbf{R}(n,t)}{\partial n^4} + \mathbf{f}(n,t). \tag{3.6}$$

In the limit of small l_p/L, normal coordinates of the form used in the Rouse model (eqn.2.8) can be used as good approximations of semiflexible polymers(Paul 97) (Krushev 02) (Guenza 03) (Bulacu 05). Thus, substituting eqn.2.11 in eqn.3.6, and multiplying by $2\cos\left(\frac{p\pi s}{L}\right)$ and integrating over n gives:

$$2L\zeta\frac{\partial}{\partial t}\tilde{\mathbf{X}}_p(t) = \frac{-6k_BT\pi^2p^2}{2Ll_p}\tilde{\mathbf{X}}_p(t) - \frac{6l_p\pi^4p^4}{2L^3}\tilde{\mathbf{X}}_p(t) + \mathbf{f}(t). \tag{3.7}$$

This leads to the effective equation,

$$\zeta_p\frac{\partial}{\partial t}\tilde{\mathbf{X}}_p(t) = -k_p^{semi}\tilde{\mathbf{X}}_p(t) + \mathbf{f}(t) \tag{3.8}$$

where the force constant is:

$$k_p^{semi} = \left(3k_BTl_p\pi^4p^4\right)/L^3 + \left(3k_BT\pi^2p^2\right)/(Ll_p)$$

Since eqn.3.8 is decoupled for each p, the correlation of the normal coordinates gives,

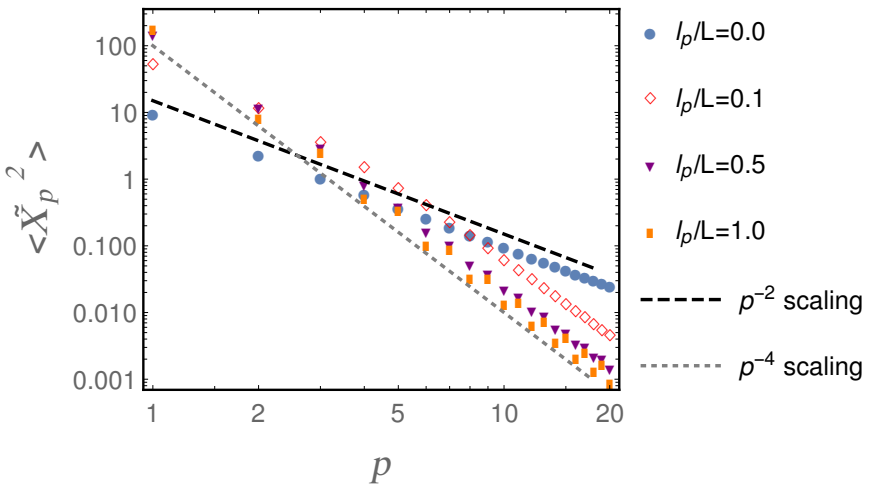

Figure 3.3: $\langle \tilde{\mathbf{X}}_p^2(0) \rangle$ as a function of p, for a 75 monomer long polymer, with increasing stiffness(l_p/L). The dashed lines correspond to the ideal Rouse and p^{-4} scaling, which respresent the two terms in eqn.3.10. The flexible case, $l_p/L = 0$ conforms to the p^{-2} scaling, whereas the stiffer chains have a p^{-4} dependence.

$$\left\langle \tilde{\mathbf{X}}_p(t) \cdot \tilde{\mathbf{X}}_p(0) \right\rangle = \left\langle \tilde{\mathbf{X}}_p^2(0) \right\rangle e^{-t/\tilde{\tau}_p},$$

where the correlation relaxation time is given by,

$$\tilde{\tau}_p = \frac{\zeta_p}{k_p^{semi}} = \left[\frac{3k_B T \pi^2}{2L^2 \zeta l_p} p^2 + \frac{3k_B T l_p \pi^4}{2NL^3 \zeta} p^4 \right]^{-1}, \tag{3.9}$$

and the mean-square mode amplitude, $\langle \tilde{\mathbf{X}}_p^2(0) \rangle$ is

$$\langle \tilde{\mathbf{X}}_p^2(0) \rangle = \frac{k_B T}{k_p^{semi}} = \left[\frac{3\pi^2}{L l_p} p^2 + \frac{3 l_p \pi^4}{L^3} p^4 \right]^{-1}. \tag{3.10}$$

The scaling of the mean-square mode amplitude with p is shown in Fig.3.3, for different l_p/L values. An increase in this ratio is a consequence of increasing the bending rigidity. The dependence for a purely flexible polymer of 75 monomers is also plotted along with that of semiflexible polymers, along with lines corresponding to pure p^{-2} and p^{-4} dependence. The flexible polymer follows the Rouse prediction of p^{-2}, as was previously shown in Fig.2.2. However, as bending rigidity is introduced, there is a clear shift towards the p^{-4} scaling. This difference in scaling can be seen to become more pronounced as the l_p/L increases. However the p^{-2} dependence can be seen in the polymer chain with l_p/L as 0.1 for the first few modes, which then transitions to

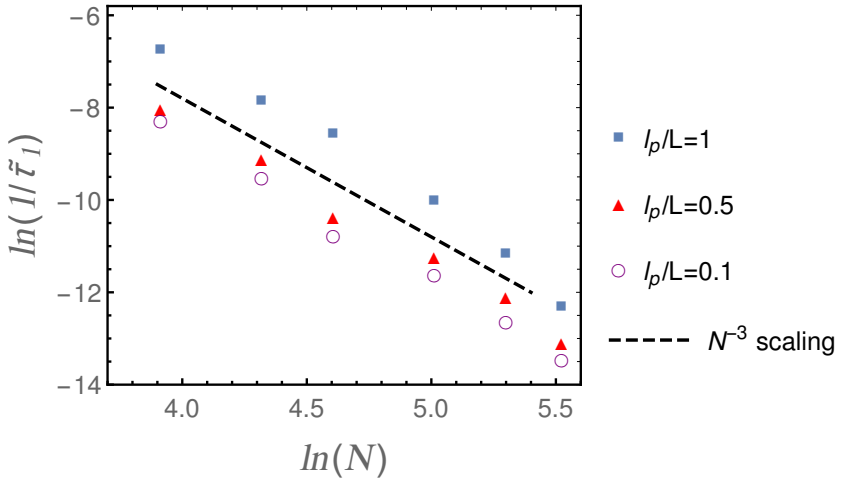

Figure 3.4: $\ln(1/\tilde{\tau}_1)$ as a function of $\ln(N)$ plotted for different l_p/L. The dashed line represents an N^{-3} scaling, followed by all the chains, as predicted by eqn.3.11.

a p^{-4} scaling as the mode number increases. This shift in scaling suggests that the normal mode treatment for small l_p/L with simultaneous quadratic and biquadratic p dependence is justified, *a posteriori*.

Using a fixed ratio of l_p/L in eqn.3.9 and assuming that the contour length $L \propto N$ gives,

$$\tilde{\tau}_p = \frac{\zeta_p}{k_p^{semi}} = \left[\frac{3k_BT\pi^2}{2L^3\zeta}\left(\frac{L}{l_p}\right)p^2 + \frac{3k_BT\pi^4}{2NL^2\zeta}\left(\frac{l_p}{L}\right)p^4\right]^{-1}$$

$$\tilde{\tau}_p = \frac{\zeta_p}{k_p^{semi}} = \left[\frac{3k_BT\pi^2}{2N^3l^3\zeta}\left(\frac{L}{l_p}\right)p^2 + \frac{3k_BT\pi^4}{2N^3l^3\zeta}\left(\frac{l_p}{L}\right)p^4\right]^{-1} \implies \tilde{\tau}_p \propto N^3. \tag{3.11}$$

This scaling can be seen in Fig.3.4, where $\ln(1/\tilde{\tau}_1)$ is plotted as a function of $\ln(N)$ for different l_p/L. The N^3 scaling is pronounced even for polymers with persistence lengths of the order of the order of the contour length, which is much greater than the low bending rigidity regime where the treatment by Steinhauser is believed to hold. However, the scaling of $\tilde{\tau}_p$ with p, is sensitive to the rigidity of the polymer chain, as can be seen in Fig.3.5. There is a clear deviation from the theoretical prediction(eqn.3.9) for higher modes in the larger l_p/L case, suggesting the limitation of the normal coordinate treatment to low values of l_p/L. An additional factor of 0.25 to the term biquadratic in p is required to make the theoretical value of $\tilde{\tau}_p$ conform with the simulation data. The origin of this factor is yet to be determined. τ_p as a function of p for a 75 monomer long flexible polymer has also been plotted along with

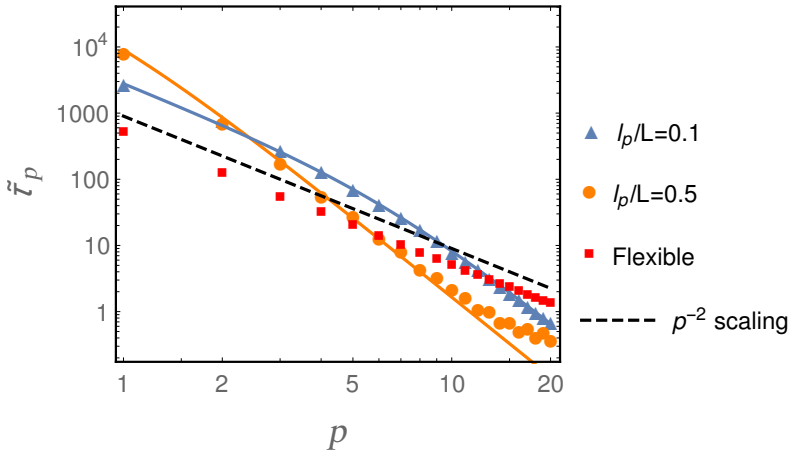

Figure 3.5: $\tilde{\tau}_p$ as a function of mode number p for a 75 monomer polymer, for different values of l_p/L. The solid lines correspond to the theoretical prediction of eqn.3.9, with a factor of 0.25 in the term biquadratic in p. Although the p dependence predicted by eqn.3.9 holds for lower mode numbers, there is a clear deviation in the stiffer chains, as mode number increases.

the increasingly rigid polymers, to illustrate the change in behaviour with introduction of bending rigidity. It has already been shown in Fig.2.1 that the flexible polymer follows a pure p^{-2} scaling.

Chapter 4

Patchy Polymers

The adsorption of polymer chains on heterogeneous surfaces is a long studied problem, using theoretical techniques such as variational procedures(Huber 98), computational modelling(Balazs 91) and experimental methods(Rockford 99)(Elbert 98). However, an equally interesting problem that is inspired from cellular settings is that of a polymer with differential type-dependent attractive wells along the polymer chain. Such a model is based off biopolymers like Actin with Actin binding proteins(ABPs) like fascin, filamin, spectrin, transgelin etc. at specific sites, that facilitate bundling and crosslinking onto other polymer chains(Dos Remedios 03)(Winder 05). It is presumed that this attractive *patchiness*, if distributed in adequate numbers randomly on a sufficiently long semiflexible polymer, can lead to its dynamics shifting towards that of a flexible polymer. The attractive wells add to the interplay between entropic and energetic costs of semiflexible polymers, and can possibly result in the collapse of the straight polymer into a globule or a *knotted* configuration, locked in place by the attractive patches.

4.1 Patchy flexible chains

The patchy attractive wells are applied to a flexible polymer as well, after which its force extension characteristic is analysed. The force extension of this patchy flexible polymer(Fig.4.1) that has been allowed to reach equilibrium reveals clear plateau-

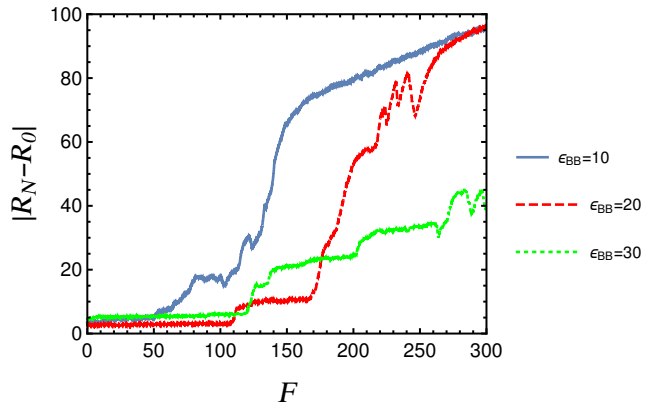

Figure 4.1: Force extension of a heterogeneous flexible polymer with varying B-B attraction strengths. $N_A/N_B = 0.5$. In all these cases, ϵ_{AA} and ϵ_{AB} is 1. The plateau-like regions correspond to the clusters preventing the extension of the polymer chain. The clustering is further visualised using the contact number plot(Fig.4.2)

.

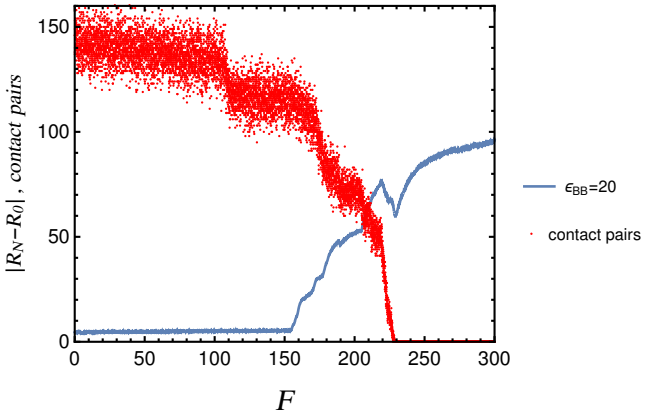

Figure 4.2: The number of contact-pairs, plotted along with the force extension plot of a collapsed heterogeneous flexible polymer chain, with $\epsilon_{BB} = 20$. The drops in contact number is indicative of the breaking of a cluster. A contact number of zero corresponds to a chain with no clusters.

like regions, which are most likely to arise from the strongly bound *knots*. Plotting the number of monomers of the same type within a cutoff of 1.1 shows the number of unique non-bonded pairs of particles within the cutoff distance in the polymer chain(Fig.4.2). When the contact number goes to zero, we can safely assume that the polymer chain is free of clusters, and should then behave like a Hookean spring, since the bonds are simply harmonic in nature. Fig.4.3 is a graphical representation of a 150 monomer long heterogeneous chain, as visualised by VMD. The figure clearly shows a cluster of type B monomers (red) that has formed in the center, with the type A monomers (black) located at the periphery of the globule.

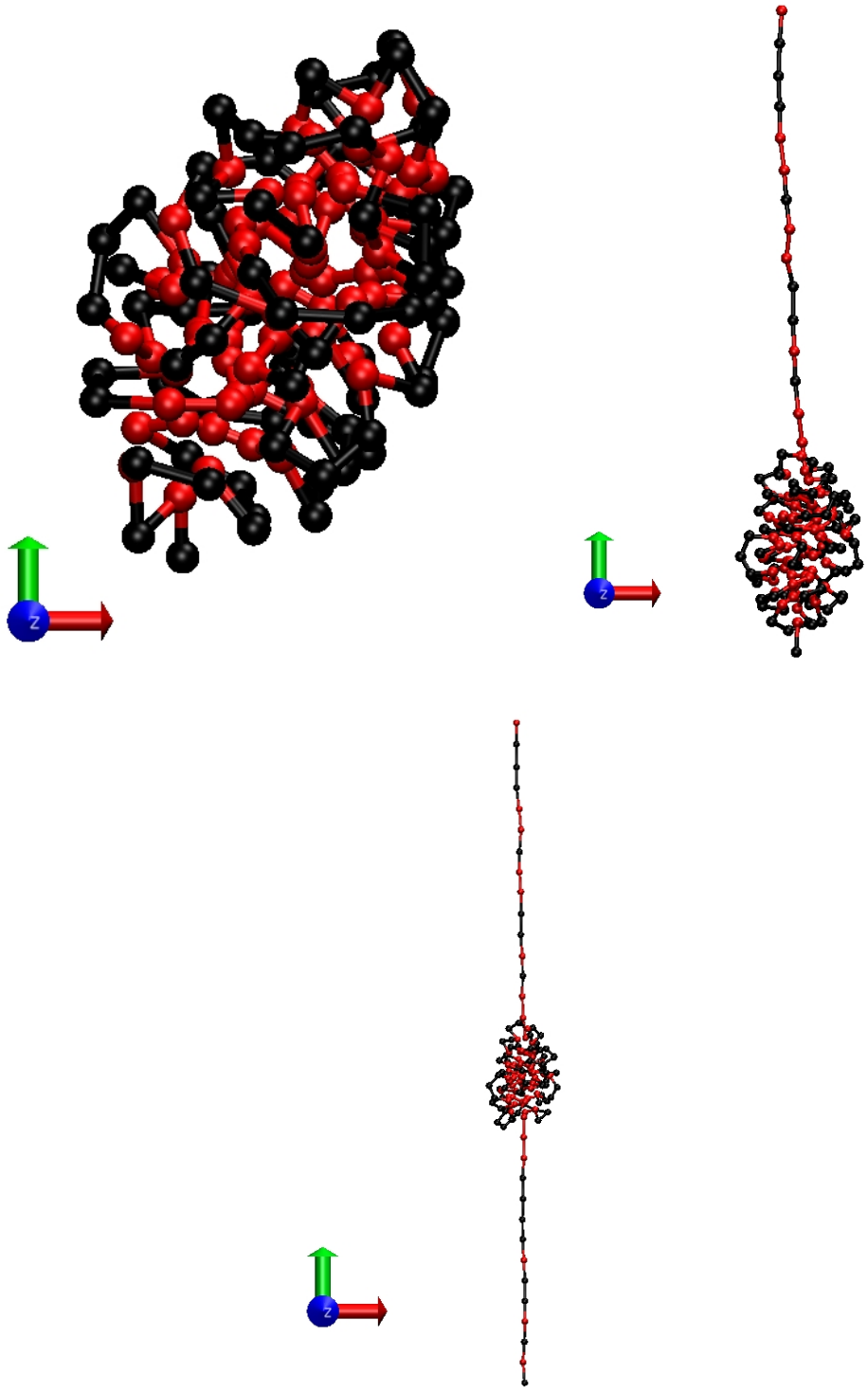

Figure 4.3: Progressive extension of a collapsed patchy 150 monomer long polymer with a pulling force applied to one end and the other end fixed. The black monomers are type B, and the red monomers are type A. $N_B/N_A = 0.5$

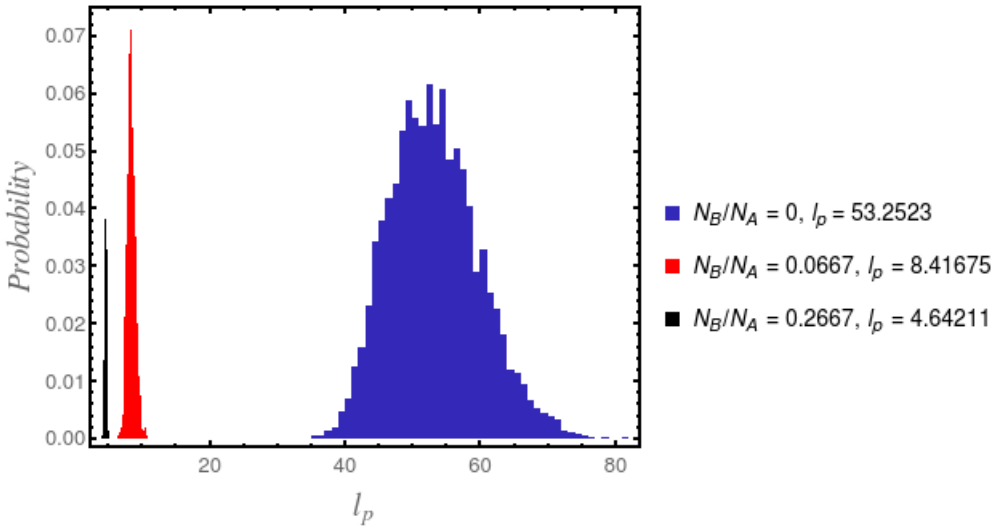

Figure 4.4: Distributions of persistence lengths of a 75 monomer semiflexible chain, with varying levels of patchiness. The bending rigidity of the chain is 75, and thus theoretical $l_p/L = 1$. There is a marked decrease in the persistence length of the chain, when random attractive patches are introduced.

4.2 Effects on semiflexible chains

Incorporating patchiness on semiflexible polymers leads to interesting observations. It is seen in Fig.4.5b that introduction of patchiness by even a small amount, $N_B/N_A = 0.0667$, leads to the chain folding up, and bound by the type B monomers. This *folding-up* effect increases with the increase in N_B/N_A, as can be seen in Fig.4.5c, where 20 type B monomers are incorporated into a 75 monomer chain. A clear difference however, visually, between the flexible and semiflexible patchy polymers, is that even though the flexible polymer forms a rather dense globule, facilitated by the absence of any bending constraints, the strong bending rigidity in the case of the semiflexible polymers renders the collapsed chain more rounded. An easily measurable quantity which can show the effects of introducing patchiness is the empirical persistence length, which can be calculated by eqn.3.2. The shift in persistence length with the introduction of patchiness can be seen in Fig.4.4, with a clear decrease in the value as patchiness is increased. A decrease in persistence length alone however, might not indicate a semiflexible to flexible shift in dynamics, and other analyses such as the normal coordinate scaling with mode number and monomer number, as employed in the previous cases, must also be used here, to arrive at a more definitive conclusion.

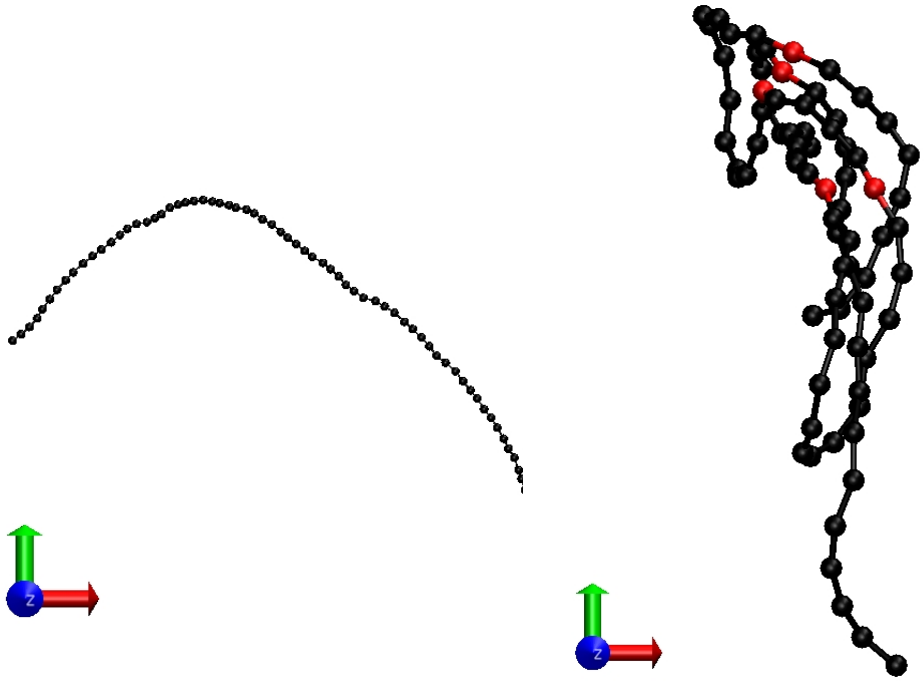

(a) $N_B/N_A = 0$ (b) $N_B/N_A = 0.0667$

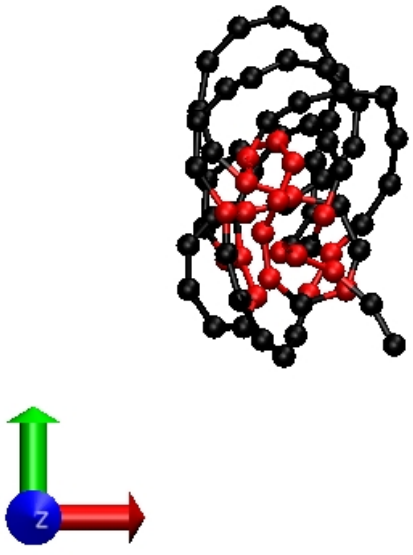

(c) $N_B/N_A = 0.2667$

Figure 4.5: 75 monomer long semiflexible polymer with varying levels of patchiness. Theoretical $l_p/L = 1$.

Chapter 5

Methodology

All the MD simulations were carried out by executing C scripts, as well as input scripts of the Large-scale Atomic/Molecular Massively Parallel Simulator (LAMMPS) (Plimpton 95), and HOOMD-Blue(Anderson 08)(Glaser 15). The primary visualization tool used was Visual Molecular Dynamics(VMD)(Humphrey 96), which was also used to carry out post processing of MD trajectories such as unwrapping over periodic boundaries and measurement of quantities such as the radius of gyration, center of mass deviation etc. The polymer chains are all bead spring systems, with point mass monomers, joined by harmonic bonds(values of parameters will be given in subsequent sections). Dimensionless units were employed, where $k_B = 1$. The timestep for all simulations was set to 0.001. The values were all dumped in a LAMMPS trajectory(C-scripts) or GSD(HOOMD-Blue) format every hundred timesteps. Thus, the data values are all 0.1 time units apart. The first twenty normal modes were computed for each timestep using eqn.2.9, after which the autocorrelation of normal modes was computed using the algorithm proposed by Likhtman, Sukumaran and Ramirez(Ramírez 07). Python3, R(R Core Team 18) and Mathematica(Inc. 18) were used at various stages of data processing, and Mathematica was used for creating all the plots.

5.1 Integrator

The Euler-Maruyama algorithm(Maruyama 55) was used to carry out simulations in the over-damped Brownian regime. Discretising eqn.2.10 using a forward difference scheme, we get:

$$\mathbf{R}_n(t+\Delta t) = \mathbf{R}_n(t) - \frac{\Delta t}{\zeta}\nabla U + \frac{\sqrt{2k_BT\Delta t}}{\zeta}\omega(t), \tag{5.1}$$

where $\omega(t)$ is a Gaussian random number with zero mean and unit variance, and is also an example of a Wiener process.
The Gaussian random variable was obtained using the polar method described by Marsaglia and Bray(Marsaglia 64). In the three dimensional case, three such random numbers were generated for each of the three Cartesian coordinates.
U contains all the bonded and non-bonded potential terms, and the forces were calculated in the lab frame.

5.2 Flexible polymers

The flexible polymer was initiated as a straight configuration of monomers, with the equilibrium separation $l = 1$. The bonds were set to be harmonic in nature, and of the form of eqn.2.6. The force constant of the bond, $k = 3k_BT$, and $T = 1$. The Euler-Maruyama integrator(eqn.5.1) was employed as the Brownian thermostat. All non-bonded interactions such as inter-particle, excluded volume, and hydrodynamic interactions were disregarded, thus representing a polymer in an implicit solvent in Θ conditions. The absence of non-bonded interactions deemed the use of periodic boundary conditions unnecessary. The system was constructed through a C-script and executed with MPI, and no GPU support. All correlations were computed after discarding the first 25×10^5 timesteps, by which the system is found to reach equilibrium, indicated by a minimization of total energy of the system.

Even though a center-of-mass based harmonic potential is employed by Doi and Edwards(Doi 88), a potential where the harmonic potential is minimum at an equilib-

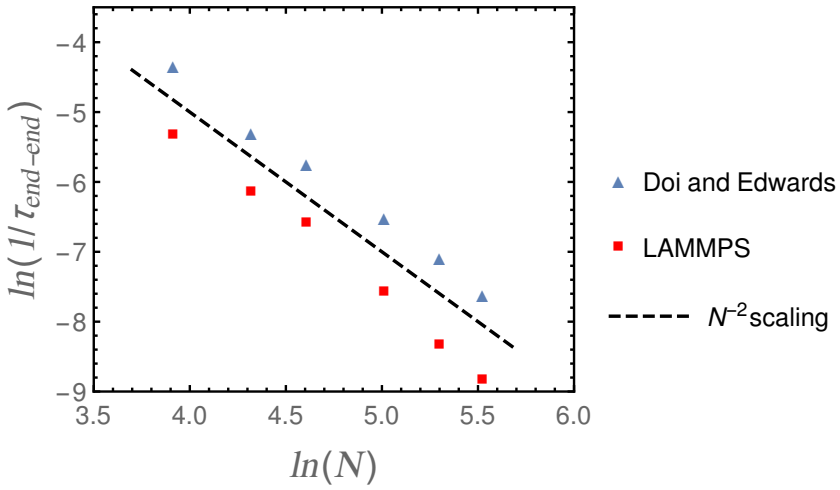

Figure 5.1: $\ln(1/\tau_{end-end})$ plotted as a function of $\ln(N)$. The dashed line shows the Rouse scaling $\propto N^{-2}$. This scaling is followed irrespective of the form of the potential (U_{bend}) used.

rium displacement equivalent to l, and is obtained from the LAMMPS(Plimpton 95) source code was used in this case, due to its ease of implementation to a variety of problems. The form of the potential affects the force that is computed as can be clearly seen in Fig.5.1. However, although there is a numerical difference between the values observed in the case of the relaxation time of the end-to-end vector correlation, its scaling with monomer number is preserved.

5.3 Dissipative Particle Dynamics

A DPD thermostat was used in order to observe Zimm scaling of the end-to-end vector correlation relaxation time. A periodic boundary simulation box large enough to prevent the interaction of the polymer chain with its instances in adjacent boxes was created, and a polymer similar to the one used in the sect.5.2 was created near the center. The simulation box was populated with individual solvent particles, located unit distance apart from each other, such that the number density of particles in the simulation box, $\rho = 1$. In order to distinguish between the monomers and the solvent particles, they were created as different types, such that the polymer was made up of type A monomers and solvent particles were type B entities. The advantage of the attribution of types to constituents of the system is the possibility of introducing type based interactions, which will play a critical role in the setting up of systems such

as that of the patchy polymer. The thermostat employed in this case was the DPD thermostat, which had the parameters a_{ij} and γ_{ij}, that had to be defined for each pair of particles i, j. Since only the effects of introducing explicit solvent particles that mimic hydrodynamic interactions through repulsive interactions with monomers and themselves were being probed, the parameters were set to, $a_{AA} = 0$, $a_{BB} = a_{AB} = 1.0$, $\gamma_{AA} = \gamma_{AB} = \gamma_{BB} = 1.0$, and $r_c = 1.0$. A HOOMD-Blue input script was written, in which the DPD interaction was invoked(Phillips 11) with the parameters as mentioned above, and run for 3×10^7 timesteps with GPU support, using a Tesla K20c card. The MD trajectory was in a GSD format, which was accessed using VMD, and was then unwrapped using built-in functions. Separate TCL scripts were sourced through VMD's Tk Console, to obtain end-to-end vectors in every frame. The normalized correlation of the end-to-end vector was fitted to the exponential series in eqn.2.16 truncated after the first five terms, in order to obtain the correlation relaxation time.

5.4 Semiflexible polymers

Semiflexible polymers were modelled as a simple extension to flexible polymers, by introducing an additional cosine potential term, which depends on the angle between two bonds. This potential is of the form of eqn.3.1, and the equilibrium bond angle was set to be π. The angular potential term was also incorporated from the LAMMPS source into a custom C-script. The bending rigidity κ was set such that the theoretical persistence length, which in equilibrium has the value κ/k_BT, took up a value so that the theoretical l_p/L was as required. For example, for a 150 monomer long chain($L = 150$) to have a theoretical l_p/L value of 0.1, κ is set to 15. Determining the average persistence length from the trajectory, using Eqn.3.2, resulted in a distribution, (Fig.3.2), centered around the empirical persistence length of the chain. This value does not necessarily conform to theoretical values for the cosine angle potential (eqn.3.5) given in (Zhang 19). Although the WLC model demands for an inextensible polymer chain, which is mathematically equivalent to maintaining unit magnitude of the tangent vector, implementation of rigid bonds is a computationally heavy task. Moreover, absolute rigidity of bonds is rather unrealistic, and so a stiff harmonic bond was instead employed. The force constant of this bond was set to $300k_BT$, with $T = 1$.

This ensured that bond length fluctuations were of the order of $\sim 1/100$. It is recommended that the ratio of the force constant to the bending rigidity is maintained at a constant value, so as to keep any effects on dynamics arising from relative strengths of bending and stretching constant throughout various simulations.

5.5 Patchy polymers

Patchiness was introduced by invoking a random number generator in the HOOMD-Blue input script to pick out particle IDs randomly, and then setting those particles as a type(type B) different from that of the rest of the monomers(type A). Particles were allowed to interact via a Lennard-Jones(LJ) potential, with the parameters $\epsilon_{AA} = \epsilon_{AB} = 1$, $\epsilon_{BB} = 10,\ 20,\ 30$, and $\sigma_{AA} = \sigma_{AB} = \sigma_{BB} = 1.0$, where the types mentioned in the subscript indicate that the parameters apply to all particles of each type. The LJ potential was cut off at distance $r_c = 2.5\sigma$, thus ensuring that the particles experienced both the attractive well as well as the repulsive close range parts of the potential. The polymer chain was tethered to a point in the simulation box by one of the terminal monomers. The force constant of the bond, was set to 300. A periodic boundary simulation box large enough to prevent the chain interacting with its instance across the periodic boundary was used, so as to mimic an isolated chain. The polymer was then subjected to a Langevin thermostat, which is the underdamped version of the Brownian thermostat, for 2×10^7 timesteps, by which it was found to equilibriate, forming a globule, with most of the type B monomers located in the center, and locked in because of the strong B-B interactions. A force was then applied to the free terminal end of the chain, which increased with each timestep. The maximum force was set to 300, and was attained at the end of 10^6 timesteps. Thus, each timestep i corresponded to a pulling force of $300i/10000$. The contact number plot of Fig.4.2 was obtained after unwrapping the trajectories in VMD, and using the built-in *measure contacts* function to determine the non-bonded pairs of particles satisfying a particular condition("type B" in this case), within a cutoff of a particle of interest(a "type B" monomer in this case). The cutoff was set to 1.1.

Simulation of a patchy semiflexible polymer chain was achieved by introducing an

additional cosine bending potential by invoking the same in the HOOMD-Blue input script. The number of monomers was set to 75, and the bending rigidity, κ was set to 75, thus making the theoretical $l_p/L = 1$. The number of type B monomers were varied, to change the level of patchiness, as 5, 10, and 20. An LJ potential was allowed to act between particles, with $\epsilon_{AA} = \epsilon_{AB} = 1$, $\epsilon_{BB} = 10$, and $\sigma_{AA} = \sigma_{AB} = \sigma_{BB} = 1.0$. The simulation was run for 2×10^7 timesteps, after which the trajectories were unwrapped in VMD, and a TCL script which measures the persistence length, averaged over the chain for each timestep using eqn.3.2, was executed through the Tk console. The persistence lengths were then binned to give Fig.4.4.

Bibliography

[Anderson 08] Joshua A Anderson, Chris D Lorenz & Alex Travesset. *General purpose molecular dynamics simulations fully implemented on graphics processing units.* Journal of computational physics, vol. 227, no. 10, pages 5342–5359, 2008.

[Auhl 03] Rolf Auhl, Ralf Everaers, Gary S Grest, Kurt Kremer & Steven J Plimpton. *Equilibration of long chain polymer melts in computer simulations.* The Journal of chemical physics, vol. 119, no. 24, pages 12718–12728, 2003.

[Balazs 91] Anna C Balazs, Kanglin Huang, Pamela McElwain & James E Brady. *Polymer adsorption on laterally heterogeneous surfaces: a Monte Carlo computer model.* Macromolecules, vol. 24, no. 3, pages 714–717, 1991.

[Beuwer 16] Michael A Beuwer, MF Knopper, Lorenzo Albertazzi, Daan van der Zwaag, Wouter G Ellenbroek, EW Meijer, Menno WJ Prins & Peter Zijlstra. *Mechanical properties of single supramolecular polymers from correlative AFM and fluorescence microscopy.* Polymer Chemistry, vol. 7, no. 47, pages 7260–7268, 2016.

[Broedersz 14] Chase P Broedersz & Fred C MacKintosh. *Modeling semiflexible polymer networks.* Reviews of Modern Physics, vol. 86, no. 3, page 995, 2014.

[Bulacu 05] Monica Bulacu & Erik van der Giessen. *Effect of bending and torsion rigidity on self-diffusion in polymer melts: A molecular-*

dynamics study. The Journal of chemical physics, vol. 123, no. 11, page 114901, 2005.

[Chu 06] Jhih-Wei Chu & Gregory A Voth. *Coarse-grained modeling of the actin filament derived from atomistic-scale simulations*. Biophysical journal, vol. 90, no. 5, pages 1572–1582, 2006.

[Dhar 02] Abhishek Dhar & Debasish Chaudhuri. *Triple minima in the free energy of semiflexible polymers*. Physical review letters, vol. 89, no. 6, page 065502, 2002.

[Doi 88] Masao Doi & Samuel Frederick Edwards. The theory of polymer dynamics, volume 73. oxford university press, 1988.

[Dos Remedios 03] CG Dos Remedios, D Chhabra, M Kekic, IV Dedova, M Tsubakihara, DA Berry & NJ Nosworthy. *Actin binding proteins: regulation of cytoskeletal microfilaments*. Physiological reviews, vol. 83, no. 2, pages 433–473, 2003.

[Dünweg 93] Burkhard Dünweg & Kurt Kremer. *Molecular dynamics simulation of a polymer chain in solution*. The Journal of chemical physics, vol. 99, no. 9, pages 6983–6997, 1993.

[Elbert 98] Donald L Elbert & Jeffrey A Hubbell. *Self-assembly and steric stabilization at heterogeneous, biological surfaces using adsorbing block copolymers*. Chemistry & biology, vol. 5, no. 3, pages 177–183, 1998.

[Glaser 15] Jens Glaser, Trung Dac Nguyen, Joshua A Anderson, Pak Lui, Filippo Spiga, Jaime A Millan, David C Morse & Sharon C Glotzer. *Strong scaling of general-purpose molecular dynamics simulations on GPUs*. Computer Physics Communications, vol. 192, pages 97–107, 2015.

[Groot 97] Robert D Groot & Patrick B Warren. *Dissipative particle dynamics: Bridging the gap between atomistic and mesoscopic simulation*.

The Journal of chemical physics, vol. 107, no. 11, pages 4423–4435, 1997.

[Guenza 03] M Guenza. *Cooperative dynamics in semiflexibile unentangled polymer fluids*. The Journal of chemical physics, vol. 119, no. 14, pages 7568–7578, 2003.

[Harnau 96] Ludger Harnau, Roland G Winkler & Peter Reineker. *Dynamic structure factor of semiflexible macromolecules in dilute solution*. The Journal of chemical physics, vol. 104, no. 16, pages 6355–6368, 1996.

[Head 03] David A Head, Alex J Levine & FC MacKintosh. *Deformation of cross-linked semiflexible polymer networks*. Physical review letters, vol. 91, no. 10, page 108102, 2003.

[Huber 98] Gregor Huber & Thomas A Vilgis. *Polymer adsorption on heterogeneous surfaces*. The European Physical Journal B-Condensed Matter and Complex Systems, vol. 3, no. 2, pages 217–223, 1998.

[Humphrey 96] William Humphrey, Andrew Dalke & Klaus Schulten. *VMD – Visual Molecular Dynamics*. Journal of Molecular Graphics, vol. 14, pages 33–38, 1996.

[Inc. 18] Wolfram Research, Inc. *Mathematica, Version 11.3*, 2018. Champaign, IL, 2018.

[Jian 97] Hongmei Jian, Alexander V Vologodskii & Tamar Schlick. *A combined wormlike-chain and bead model for dynamic simulations of long linear DNA*. Journal of Computational Physics, vol. 136, no. 1, pages 168–179, 1997.

[Kang 17] Ding Kang, Zhixiang Cai, Yue Wei & Hongbin Zhang. *Structure and chain conformation characteristics of high acyl gellan gum polysaccharide in DMSO with sodium nitrate*. Polymer, vol. 128, pages 147–158, 2017.

[Kratky 49] O Kratky & G Porod. *Röntgenuntersuchung gelöster faden-*

molekül. Recueil des Travaux Chimiques des Pays-Bas, vol. 68, no. 12, pages 1106–1122, 1949.

[Kroy 96] Klaus Kroy & Erwin Frey. *Force-extension relation and plateau modulus for wormlike chains*. Physical review letters, vol. 77, no. 2, page 306, 1996.

[Kroy 07] Klaus Kroy & Jens Glaser. *The glassy wormlike chain*. New Journal of Physics, vol. 9, no. 11, page 416, 2007.

[Krushev 02] S Krushev, W Paul & GD Smith. *The role of internal rotational barriers in polymer melt chain dynamics*. Macromolecules, vol. 35, no. 10, pages 4198–4203, 2002.

[Langevin 08] Paul Langevin. *Sur la théorie du mouvement brownien*. Comptes rendus de l'Académie des Sciences, vol. 146, pages 530–533, 1908.

[Lax 60] Melvin Lax. *Fluctuations from the nonequilibrium steady state*. Reviews of modern physics, vol. 32, no. 1, page 25, 1960.

[Marko 95] John F Marko & Eric D Siggia. *Stretching dna*. Macromolecules, vol. 28, no. 26, pages 8759–8770, 1995.

[Marsaglia 64] George Marsaglia & Thomas A Bray. *A convenient method for generating normal variables*. SIAM review, vol. 6, no. 3, pages 260–264, 1964.

[Maruyama 55] Gisiro Maruyama. *Continuous Markov processes and stochastic equations*. Rendiconti del Circolo Matematico di Palermo, vol. 4, no. 1, pages 48–90, 1955.

[Mazur 07] Alexey K Mazur. *Wormlike chain theory and bending of short DNA*. Physical review letters, vol. 98, no. 21, page 218102, 2007.

[Nikoubashman 16] Arash Nikoubashman, Andrey Milchev & Kurt Binder. *Dynamics of single semiflexible polymers in dilute solution*. The Journal of chemical physics, vol. 145, no. 23, page 234903, 2016.

[Noda 81] Ichiro Noda, Narundo Kato, Toshiaki Kitano & Mitsuru Nagasawa.

Thermodynamic properties of moderately concentrated solutions of linear polymers. Macromolecules, vol. 14, no. 3, pages 668–676, 1981.

[Paul 97] W Paul, Grant D Smith & Do Y Yoon. *Static and dynamic properties of an-C100H202 melt from molecular dynamics simulations.* Macromolecules, vol. 30, no. 25, pages 7772–7780, 1997.

[Phillips 11] Carolyn L Phillips, Joshua A Anderson & Sharon C Glotzer. *Pseudo-random number generation for Brownian Dynamics and Dissipative Particle Dynamics simulations on GPU devices.* Journal of Computational Physics, vol. 230, no. 19, pages 7191–7201, 2011.

[Plimpton 95] Steve Plimpton. *Fast parallel algorithms for short-range molecular dynamics.* Journal of computational physics, vol. 117, no. 1, pages 1–19, 1995.

[R Core Team 18] R Core Team. *R: A Language and Environment for Statistical Computing.* R Foundation for Statistical Computing, Vienna, Austria, 2018.

[Ramírez 07] Jorge Ramírez, Sathish K Sukumaran & Alexei E Likhtman. *Significance of cross correlations in the stress relaxation of polymer melts.* The Journal of chemical physics, vol. 126, no. 24, page 244904, 2007.

[Rockford 99] L Rockford, Y Liu, P Mansky, TP Russell, M Yoon & SGJ Mochrie. *Polymers on nanoperiodic, heterogeneous surfaces.* Physical review letters, vol. 82, no. 12, page 2602, 1999.

[Rouse Jr 53] Prince E Rouse Jr. *A theory of the linear viscoelastic properties of dilute solutions of coiling polymers.* The Journal of Chemical Physics, vol. 21, no. 7, pages 1272–1280, 1953.

[Schuldt 16] Carsten Schuldt, Jörg Schnauß, Tina Händler, Martin Glaser, Jessica Lorenz, Tom Golde, Josef A Käs & David M Smith. *Tuning*

synthetic semiflexible networks by bending stiffness. Physical review letters, vol. 117, no. 19, page 197801, 2016.

[Seymour 03] Raymond Benedict Seymour & Charles E Carraher. Seymour/carraher's polymer chemistry. M. Dekker, 2003.

[Skolnick 77] Jeffrey Skolnick & Marshall Fixman. *Electrostatic persistence length of a wormlike polyelectrolyte.* Macromolecules, vol. 10, no. 5, pages 944–948, 1977.

[Spaeth 11] Justin R Spaeth, Ioannis G Kevrekidis & Athanassios Z Panagiotopoulos. *A comparison of implicit-and explicit-solvent simulations of self-assembly in block copolymer and solute systems.* The Journal of chemical physics, vol. 134, no. 16, page 164902, 2011.

[Staudinger 20] Hermann Staudinger. *Über polymerisation.* Berichte der deutschen chemischen Gesellschaft (A and B Series), vol. 53, no. 6, pages 1073–1085, 1920.

[Steinhauser 08] Martin O Steinhauser. *Static and dynamic scaling of semiflexible polymer chains—a molecular dynamics simulation study of single chains and melts.* Mechanics of Time-Dependent Materials, vol. 12, no. 4, page 291, 2008.

[Tassieri 08a] M Tassieri, RML Evans, L Barbu-Tudoran, J Trinick & TA Waigh. *The self-assembly, elasticity, and dynamics of cardiac thin filaments.* Biophysical journal, vol. 94, no. 6, pages 2170–2178, 2008.

[Tassieri 08b] Manlio Tassieri, RML Evans, Lucian Barbu-Tudoran, G Nasir Khaname, John Trinick & Tom A Waigh. *Dynamics of semiflexible polymer solutions in the highly entangled regime.* Physical review letters, vol. 101, no. 19, page 198301, 2008.

[Tassieri 17] Manlio Tassieri. *Dynamics of semiflexible polymer solutions in the tightly entangled concentration regime.* Macromolecules, vol. 50, no. 14, pages 5611–5618, 2017.

[Winder 05] Steven J Winder & Kathryn R Ayscough. *Actin-binding proteins.* Journal of cell science, vol. 118, no. 4, pages 651–654, 2005.

[Yang 02] Shilong Yang, James B Witkoskie & Jianshu Cao. *Single-molecule dynamics of semiflexible Gaussian chains.* The Journal of chemical physics, vol. 117, no. 24, pages 11010–11023, 2002.

[Zhang 19] Jing-Zi Zhang, Xiang-Yao Peng, Shan Liu, Bang-Ping Jiang, Shi-Chen Ji & Xing-Can Shen. *The Persistence Length of Semiflexible Polymers in Lattice Monte Carlo Simulations.* Polymers, vol. 11, no. 2, page 295, 2019.

[Zimm 56] Bruno H Zimm. *Dynamics of polymer molecules in dilute solution: viscoelasticity, flow birefringence and dielectric loss.* The journal of chemical physics, vol. 24, no. 2, pages 269–278, 1956.